DFT, anticancer, antioxidant and molecular docking investigations of some ternary Ni(II) complexes with 2-[(E)-[4-(dimethylamino)phenyl]methyleneamino]pi

Ranjan K. Mohapatra, Marei M. El-ajaily, Faten S. Alassbaly, Ashish K. Sarangi, Debadutta Das, Abdussalam A. Maihub, et al.

Chemical Papers

ISSN 2585-7290
Volume 75
Number 3

Chem. Pap. (2021) 75:1005-1019
DOI 10.1007/s11696-020-01342-8

Springer

Chemical Papers (2021) 75:1005–1019
https://doi.org/10.1007/s11696-020-01342-8

ORIGINAL PAPER

DFT, anticancer, antioxidant and molecular docking investigations of some ternary Ni(II) complexes with 2-[(E)-[4-(dimethylamino) phenyl]methyleneamino]phenol

Ranjan K. Mohapatra[1] · Marei M. El-ajaily[2] · Faten S. Alassbaly[2] · Ashish K. Sarangi[3] · Debadutta Das[4] · Abdussalam A. Maihub[5] · Salha F. Ben-Gweirif[6] · Ahmed Mahal[7,8] · Marharyta Suleiman[9] · Lina Perekhoda[9] · Mohammad Azam[10] · Taghreed H. Al-Noor[11]

Received: 17 May 2020 / Accepted: 31 August 2020 / Published online: 23 September 2020

Abstract

The biological activities of some ternary nickel complexes with a Schiff base obtained from 4-dimethylaminobenzaldehyde and 2-aminophenol have been reported. The Schiff base (HL_1) acts as a primary ligand whereas, anthranilic acid (HL_2), 2-nitroaniline (HL_3), alanine (HL_4) and histidine (HL_5) act as secondary ligand or co-ligand. The anticancer activity of these compounds was studied against human colon carcinoma (HCT-116), human hepatocellular liver carcinoma (HEPG-2) and human breast carcinoma (MCF-7) cell lines. As per the results, the compounds were active against the cell lines. The antioxidant activity of the same compounds was evaluated using DPPH (1,1-diphenyl-2-picryl-hydrazyl) radical scavenging and compared with ascorbic acid. The DFT computations for these compounds were made to understand the bonding mode by a GAUSSIAN 09 program. Moreover, a docking analysis using Autodock 4.2 software package was carried out against the tyrosine kinase receptor (PDB ID: 1M17). In addition, QSAR investigation was also performed to understand the biological potency of the ligand.

Keywords Ternary Ni(II) complexes · DFT · Anticancer · Antioxidant · Docking studies

Electronic supplementary material The online version of this article (https://doi.org/10.1007/s11696-020-01342-8) contains supplementary material, which is available to authorized users.

✉ Ranjan K. Mohapatra
ranjank_mohapatra@yahoo.com

✉ Ashish K. Sarangi
ashishsbp_2008@yahoo.com

[1] Department of Chemistry, Government College of Engineering, Keonjhar, Odisha, India

[2] Chemistry Department, Faculty of Science, Benghazi University, Benghazi, Libya

[3] Department of Chemistry, School of Applied Sciences, Centurion University of Technology and Management, Odisha, India

[4] Department of Chemistry, Sukanti Degree College, Subarnapur, Odisha, India

[5] Chemistry department, Faculty of Science, Tripoli University, Tripoli, Libya

[6] Botany department, Faculty of Science, Benghazi University, Benghazi, Libya

[7] Key Laboratory of Plant Resources Conservation and Sustainable Utilization and Guangdong Provincial Key Laboratory of Applied Botany, South China Botanical Garden, Chinese Academy of Sciences, Guangzhou 510650, People's Republic of China

[8] Guangzhou HC Pharmaceutical Co Ltd., Guangzhou 510663, People's Republic of China

[9] Department of Medicinal Chemistry, National University of Pharmacy, Pushkinska Str. 53, Kharkiv 61002, Ukraine

[10] Department of Chemistry, College of Science, King Saud University, PO BOX 2455, Riyadh 11451, Kingdom of Saudi Arabia

[11] Chemistry Department, Ibn-Al-Haithem College of Education for Pure Science, Baghdad University, Baghdad, Iraq

Introduction

The chemistry of Schiff bases has been discussed extensively over the past few decades [Mohapatra et al. 2018a] due to their broad range of biological, biochemical and pharmacological activities. It is a commonly used organic ligand having –C=N– linkage and can coordinate to different metal ions via azomethine nitrogen. It has been reported that the presence of lone pair electron on sp^2 hybridized nitrogen atom of the –C=N– linkage is responsible for the biological properties [Patal 1970]. It has also been reported that the Schiff bases and their metal complexes have a wide range of medicinal applications, such as anti-microbial, antioxidant, anticancer, anti-HIV, anti-inflammatory activity. (El-Saghier et al. 2019; Ahamad et al. 2020; Sama et al. 2017; Kavitha and Reddy 2016) The activity is enhanced when these compounds are forming complexes with various metal ions. (Mohapatra et al. 2014, 2018b; Gaber et al. 2019; Mohapatra et al. 2019a).

Most of the divalent transition metal ions have an important role in the biological processes in the human body. The study of their coordination chemistry with mixed ligands has been one of the important developments in the field of bioinorganic chemistry (Kaim and Schwederski 1996). Over the years, ternary complexes, often referred as mixed ligand complexes have received considerable attention due to their wide role in analytical chemistry (Sigel 1975; Rao et al. 1998). However, recent studies showed that the ternary complexes with biologically potential ligands find use in various enzymatic reactions and a large number of biological studies (Sigel 1975; Fathima et al. 2019; El-ajaily et al. 2018).

This is our continuing interest to design and study the medicinal properties of new drug-like compounds (Drapak et al. 2019; Sarangi et al. 2020; El-Barasi et al. 2020). In this work, we have reported the anticancer, antioxidant and molecular docking studies of some mixed ligand nickel complexes. Moreover, DFT computations were carried out to obtain information inside into the structure.

Experimental

Material

All chemicals and reagents including 4-dimethylaminobenzaldehyde, 2-aminophenol, anthranilic acid, 2-nitroaniline, alanine, histidine and Ni(II) salt were of Sigma-Aldrich and used as such. The Schiff base ligand and its ternary Ni(II) complexes have been synthesized by literature method (Alassbaly et al. 2014; Maihub et al. 2014; El-ajaily et al. 2015; Alassbaly et al. 2016).

Measurement of cytotoxicity by SRB assay

Cell lines and culturing

The human colon carcinoma (HCT-116), human hepatocellular liver carcinoma (HEPG-2) and human breast carcinoma (MCF-7) cell lines were used for this study. These cell lines were obtained in the frozen state under liquid nitrogen (− 180 °C) and maintained by serial sub-culturing in National Cancer Institute, Cairo University, Egypt. The cells were grown in RPMI-1640 medium supplemented with 10% fetal calf serum in presence of 1% L-glutamine and 1% antibiotic mixture (10 U/ml K-penicillin, 25 µg/ml amphotericin B and 10 µg/ml streptomycin sulphate). The compounds and standard drug (Doxorubicin) were evaluated for their cytotoxic activity in RCMB, Al-Azhar University, according to SRB (Sulfo-Rhodamine B) assay (Skehan and Storeng 1990, NCCLS 2000). Cytotoxicity levels were expressed as IC_{50} values and calculated (Chudzik et al. 2015). The cells were cultured at 37 °C in a humidified incubator containing 5% CO_2 in air. Following 24, 48 and 72 h treatment, cells were fixed, washed and stained with Sulforhodamine B stain. After the incubation period, the viable cells yield was determined by a colorimetric method. The percentage cell viability was calculated using Microsoft Excel as per the formula:

$$\% \text{ Cell viability} = (\text{Mean Abs control} - \text{Mean Abs test metabolite}) \times 100$$

where Abs is the absorbance at 590 nm.

DPPH free radical scavenging activity

The antioxidant activity of these studied chelates was determined at RCMB, Al-Azhar University by DPPH free radical scavenging assay (Mantasha et al. 2019). The freshly prepared methanol solution (0.004% w/v) of 2,2-diphenyl-1-picrylhydrazyl (DPPH) radical was prepared and stored in a dark place at 10 °C. A 40 µl aliquot of methanol solution was added to 3 ml of DPPH solution. The absorbance measurements were recorded immediately using a UV–Vis spectrophotometer at 1-min intervals until the absorbance stabilized (16 min). The absorbance of DPPH radical without antioxidant (control) and ascorbic acid (reference) were also measured. The study was carried out in triplicate and

average was taken. The percentage inhibition (PI) was determined according to the formula:

$$\mathrm{PI} = \frac{(AC - AT)}{AC} \times 100$$

where AC = absorbance of the control at t = 0 min and AT = absorbance of the mixed ligand chelates + DPPH at t = 16 min.

DFT Assessment

The reported compounds were optimized and examined by Gauss View 6.0.16 graphical interface program (GaussView 2009). The DFT evaluations were carried out using GAUSSIAN 09 suit programs (Becke 1993; Lee et al. 1988; Becke 1988; Hay and Wadt 1984, 1985a, b; Frisch 2009). The very useful methods for exchange–correlation functional i.e. B3LYP is applied with 6-31 G (d, p)/LANL2DZ basic set.

Molecular docking studies

For receptor-oriented flexible docking, the Autodock 4.2 software package was used. ligands were prepared using the MGL Tools 1.5.6 program. The ligand optimization was performed using the Avogadro program. To perform calculations in the Autodock 4.2 program the output formats of the receptor and ligand data were converted to a special PDBQT format (Mantasha et al. 2019). The active macromolecule center of the tyrosine kinase receptor (PDB ID: 1M17) from the Protein Data Bank (PDB) was used as a biological target for docking. The receptor maps were made in MGL Tools and AutoGrid programs. The visual analysis in the active center of tyrosine kinase receptor (PDB ID: 1M17) was performed using Discovery Studio Visualizer program.

Results and discussion

Computational analysis

For a clear understanding of the structural characteristics of the metal ion in all complexes computational studies were performed in a GAUSSIAN program platform. The Schiff base ligand (HL_1) and its Ni(II) complexes (Figs. 1, 2, 3, 4, 6) were optimized using B3LYP/6-31 + G (d,p) and B3LYP/LANL2DZ/SSD basic set to create the geometrical structures theoretically. Few structural parameters are important to elucidate the structure of the compounds such as bond lengths and bond angles of the optimized ligand and its complexes are presented in Table 1, which prominently explained the bonding mode influence between the ligand with the metal atoms (Yousef et al. 2011, 2012a). The assessment of energetic properties such as single point energy and dipole moment (D) values of all the compounds are inspected using DFT/B3LYP 6-31 + G (d,p) and DFT/B3LYP LANL2DZ basic sets. The single point energy comparison made between the ligand and its nickel complexes, prominently suggested that the metal complexes are more stable than the free ligand (Sarangi et al. 2018, El-ajaily et al. 2019) as the complexes lie lower in energy than the (free) ligand. From the calculated data, it is also confirmed that $[NiL1L2(H_2O)_2]H_2O$ have maximum dipole–dipole interaction (Table 2).

Frontier molecular orbitals (FMO's) investigation

To understand the complexation reaction and discover the reactive site in a conjugate system FMO's studies play important roles. The molecular energies of E_{HOMO} and E_{LUMO} for the main ligand and all of its nickel complexes apparently explain the global reactivity descriptors such as chemical potential, chemical hardness and electrophilicity. The expected coordination site is clearly explained from the assessment of the molecular orbital coefficients (Yousef

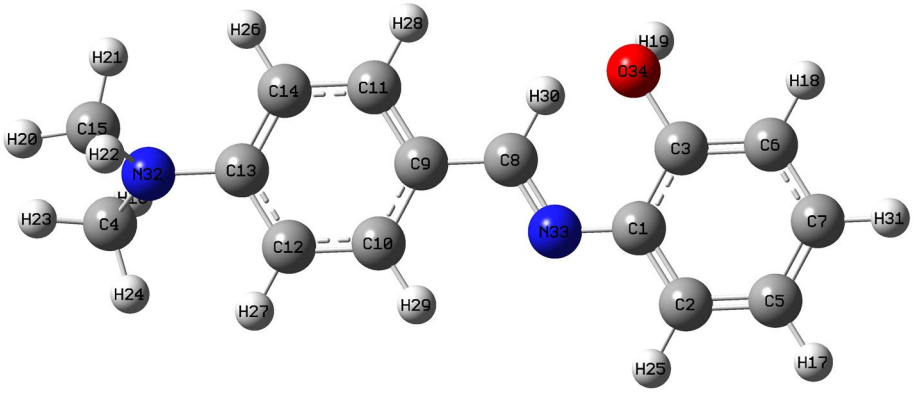

Fig. 1 Optimized geometry of the ligand (HL_1)

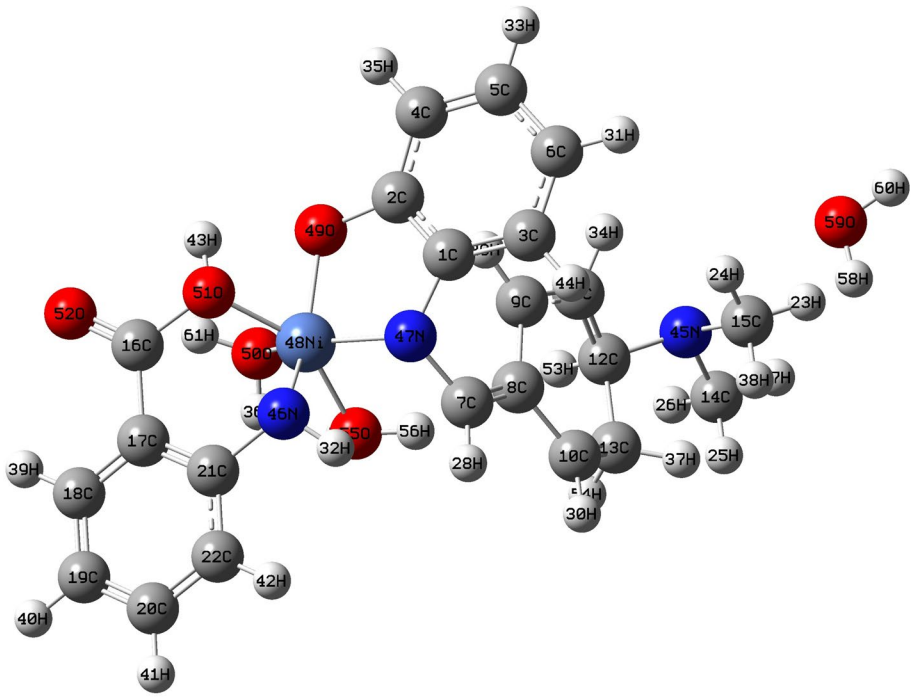

Fig. 2 Optimized geometry of $[NiL1L2(H_2O)_2]H_2O$

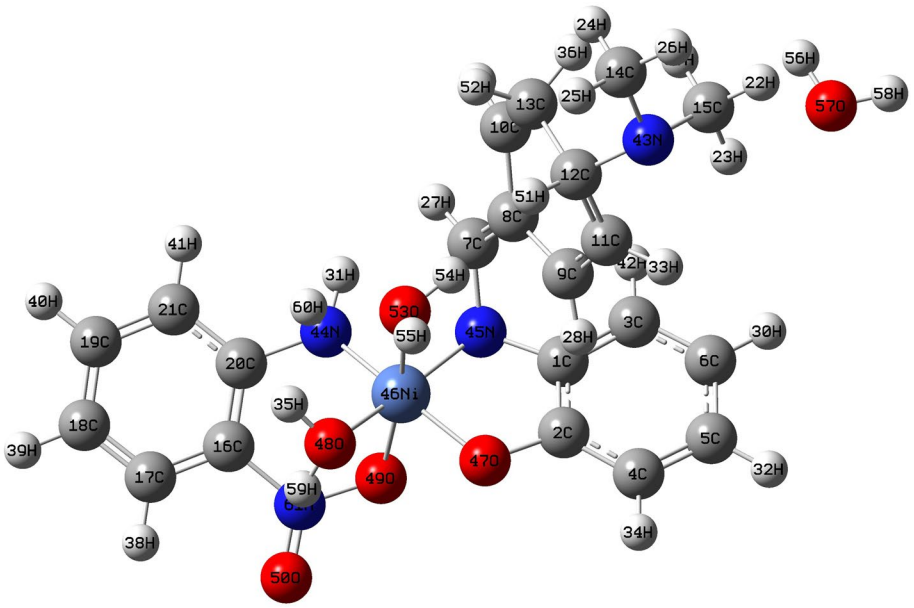

Fig. 3 Optimized geometry of $[NiL1L3(H_2O)_2]H_2O$

et al. 2012b, 2013). The negative values of the energies of E_{HOMO} and E_{LUMO} for the ligand (HL_1) and all of its Ni complexes are confirmed the stability (Yousef et al. 2013; Govindarajan et al. 2012). A near observation of the LUMO orbital electron cloud for primary ligand sharply localized the electron density on the N_{32}, N_{33} and O_{34} (Fig. 5) for favorable atomic sites in the nucleophilic attacking position. The differences in molecular energy predominantly describe the chemical reactivity and chemical stability of the strongly active molecule (Pearson 1989). The molecular orbital energy gap between HOMO and LUMO for the $[NiL1L5(H_2O)_2]2H_2O$ complex is established to be less than all the complexes and ligand. From the energy comparison values it is prominently explained that the reactivity of the $[NiL1L5(H_2O)_2]2H_2O$ complex is greater than all other complexes and free ligand (Figs. 6, 7).

For a clear understanding of FMO's, few important quantum chemical parameters such as electronegativity (χ), global hardness (η), chemical potential (μ), global softness (S) and global electrophilicity index (ω) were determined

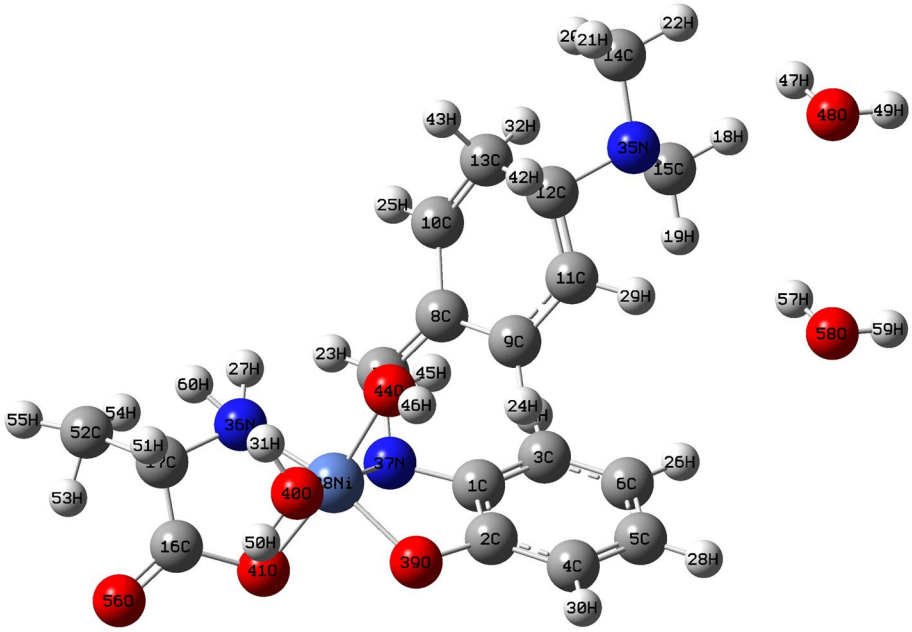

Fig. 4 Optimized geometry of $[NiL1L4(H_2O)_2]2H_2O$

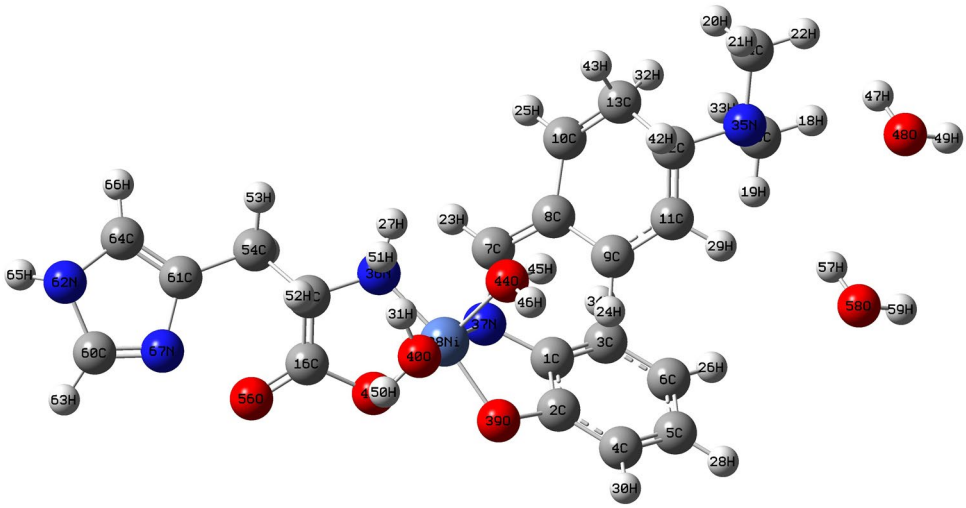

Fig. 5 Optimized geometry of $[NiL1L5(H_2O)_2]2H_2O$

(Padmanabhan et al. 2007, Pearson 1993) and presented in Table S1.

$$\chi = -\frac{(E_{LUMO} + E_{HOMO})}{2}$$

$$\mu = -\chi = \frac{(E_{LUMO} + E_{HOMO})}{2}$$

$$\eta = \frac{(E_{LUMO} - E_{HOMO})}{2}$$

$$S = \frac{1}{2\eta}$$

$$\omega = \frac{\mu^2}{2\eta}$$

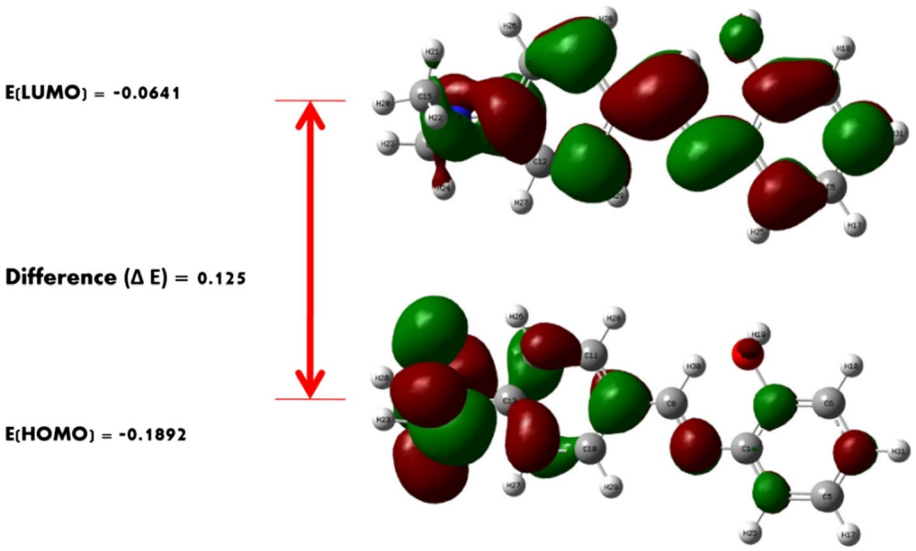

Fig. 6 HOMO−LUMO energy comparison of the ligand (HL_1)

Table 1 Optimized bond lengths and angles according to DFT calculations

$(C_{15}H_{16}N_2O_1)$ HL_1 B3LYP/6.31G (d, p)		$[NiL1L5(H_2O)_2]2H_2O$ B3LYP/LANL2DZ	
Bond length in (Å)	Bond Angle in (°)	Bond length in (Å)	Bond Angle in (°)
C1-N33 (1.301)	C1-N33-C8 (119.989)	C1-N37 (1.452)	C1-N37-C7 (110.101)
C8-N33 (1.302)	C1-C3-O34 (120.011)	C7-N37 (1.469)	C1-C2-O39 (115.382)
C3-O34 (1.409)	C1-C3-C6 (119.985)	C2-O39 (1.425)	C1-C2-C4 (120.810)
C3-C6 (1.386)	C8-C9-C11 (120.008)	C1-C2 (1.368)	C7-C8-C9 (121.408)
C8-C9 (1.386)		C2-C4 (1.398)	C1-N37-Ni38 (106.236)
		C7-C8 (1.354)	C2-N39-Ni38 (107.561)
		O39-Ni38 (1.834)	C7-N37-Ni38 (111.702)
–	–	O44-Ni38 (1.810)	C2-O39-Ni38 (107.561)
–	–	O41-Ni38 (1.843)	C17-N36-Ni38 (112.819)
–	–	N36-Ni38 (1.827)	C16-O41-Ni38 (108.649)
–	–	C17-N36 (1.445)	C16-C17-N36 (104.463)
–	–	C16-O41 (1.449)	C17-C16-O41 (115.969)
–	–	C16-C17 (1.345)	N36-Ni38-O41 (79.688)
–	–	O40-Ni38 (1.809)	N37-Ni38-O39 (79.688)
–	–	O44-Ni38 (1.810)	–

Table 2 Energetic properties of the reported compounds calculated by DFT/B3LYP 6.31 + G (d, p) and DFT/B3LYP LANL2DZ basic sets

Compound		Single point energy (kcal/mol)		Dipole moment (D)	
		DFT/B3LYP 6.31G + (d, P)	DFT/B3LYP LANL2DZ	DFT/B3LYP 6.31G + (d, P)	DFT/B3LYP LANL2DZ
Comp. 1	$(C_{15}H_{16}N_2O_1)$ HL1	-4.8060×10^6	–	0.743	–
Comp. 2	$[NiL1L2(H_2O)_2]H_2O$	-20.0617×10^6	-20.1301×10^6	1.689	1.511
Comp. 3	$[NiL1L3(H_2O)_2]H_2O$	-19.7980×10^6	-19.5681×10^6	−0.741	−0.638
Comp. 4	$[NiL1L4(H_2O)_2]2H_2O$	-19.5451×10^6	-19.3791×10^6	1.311	1. 287
Comp. 5	$[NiL1L5(H_2O)_2]2H_2O$	-20.9687×10^6	-20.7492×10^6	−1.684	−1.581

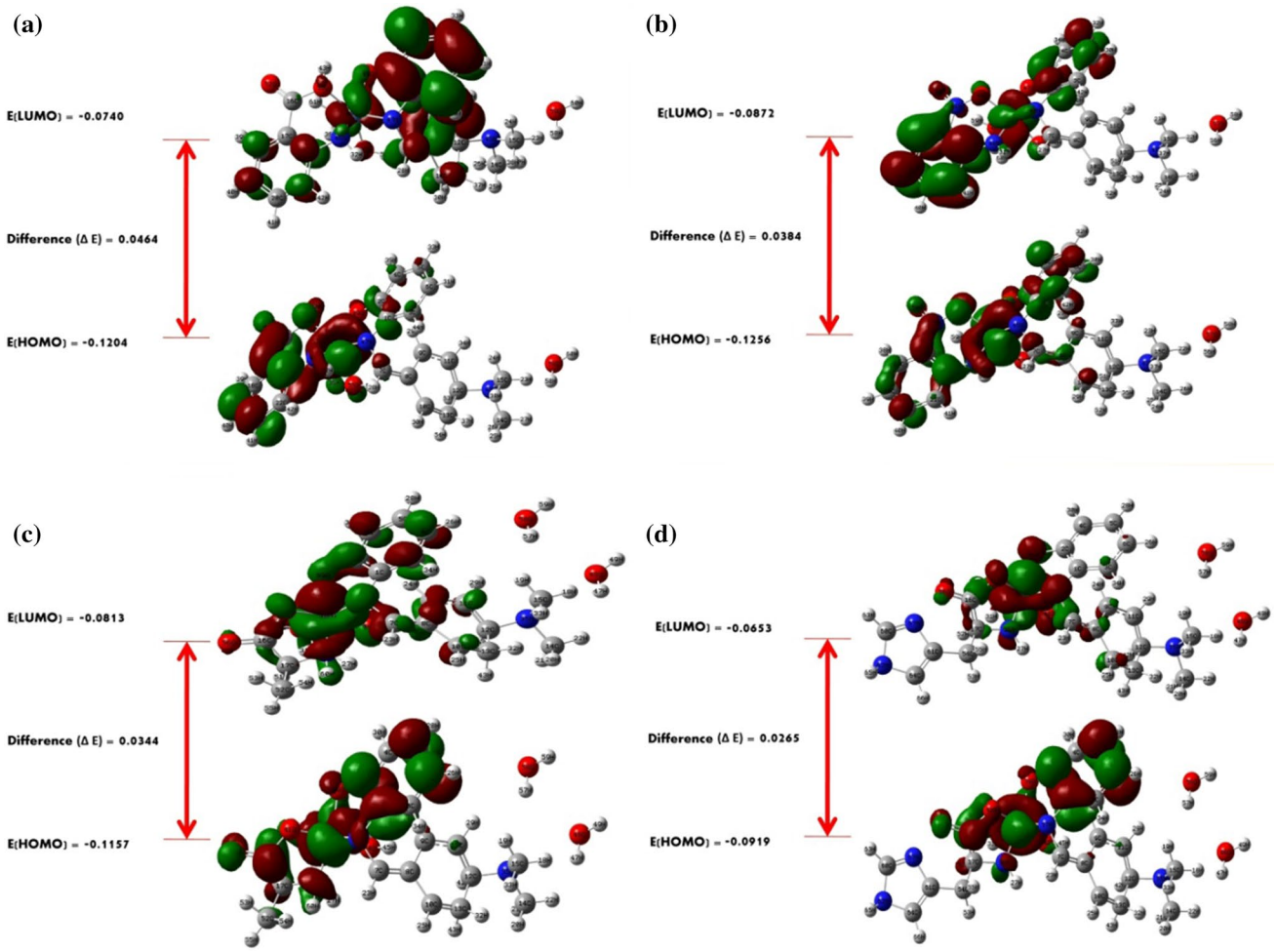

Fig. 7 HOMO–LUMO energy comparison of **a** $[NiL1L2(H_2O)_2]H_2O$, **b** $[NiL1L3(H_2O)_2]H_2O$, **c** $[NiL1L4(H_2O)_2]2H_2O$, **d** $[NiL1L5(H_2O)_2]2H_2O$

$$\sigma = \frac{1}{\eta}$$

Such analyses are helpful to describe the chemical reactivity of the compound and the identification of the reactive sites in the molecular system. The energy difference between the highest occupied molecular orbital's and lowest unoccupied molecular orbital's level clearly explaining the charge-transfer interaction. The two important quantum chemical parameters as global hardness and global softness predicted from the band energy between HOMO–LUMO orbitals i.e. hard molecule large bandgap and soft molecule small bandgap (Pearson 1993). If we compare the chemical softness (S) of the ligand is less than all Ni(II) complexes, therefore, the reactivity of the ligand grater than all complex. Further some key parameter, such as the electrophilicity (ω), assign a positive value, which quantifies the tendency of the system to accept an electron from the surrounding that clearly explains the complexes are more stable than the free ligand (Table S1).

In vitro anticancer activity

The in vitro growth inhibitory activity of the prepared ternary Ni(II) complexes was evaluated against HCT-116, HEPG-2 and MCF-7 cell lines along with the standard anticancer drug doxorubicin to assess cell proliferation. The inhibitory activities of comp. 5 against HEPG-2 cell lines were shown in Fig. 8. The IC_{50} values of the tested compounds were determined and compared with doxorubicin (Aljahdali et al. 2014). We know, the compounds exhibited IC_{50} value below 5.00 µg/ml, within the range of 5.00–10.00 µg/ml and 10.00–25.00 µg/ml are considered strong, moderate and weak anticancer agents, respectively (Shier 1991; Gaber et al. 2017). The obtained data showed that compound 3 and 4 were found to be more potent against all cancer cell lines, whereas, compound 2 and 5 were found to be moderately active. The inhibitory activities of compound 4 against hepatocellular liver carcinoma (HEPG-2) cell lines are shown in Fig. 9.

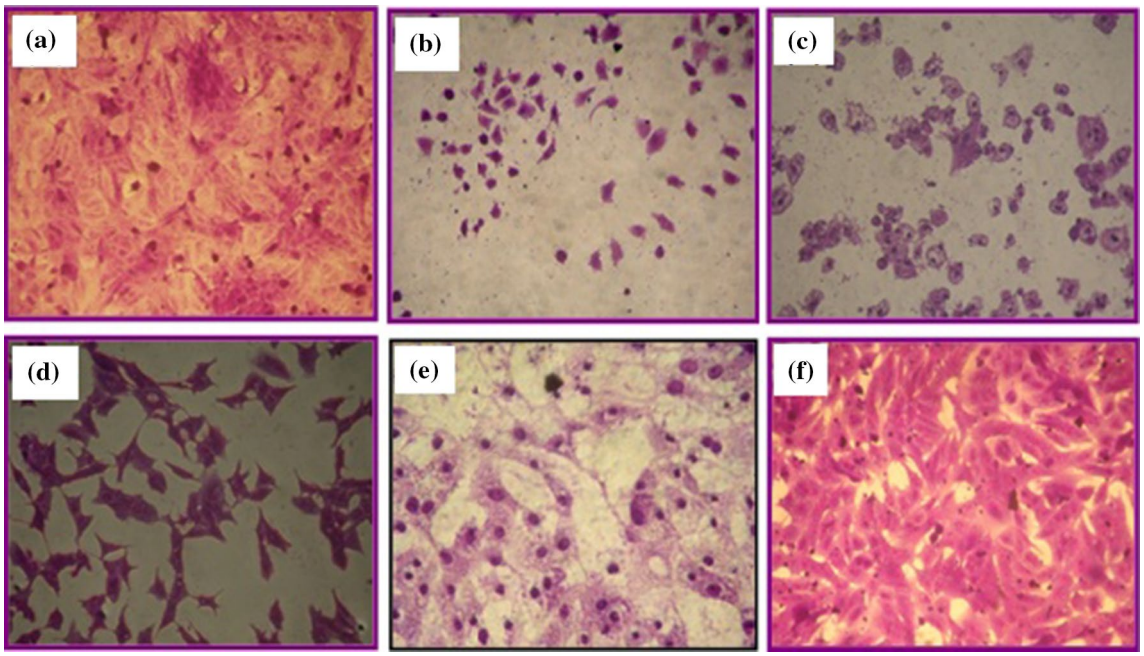

Fig. 8 Inhibitory activities of compound-5 against hepatocellular carcinoma (HEPG-2) cell lines (**a** HEPG-2 non treated; **b** treated at 25µg/ml; **c** treated at 12.50 µg/ml; **d** treated at 6.25 µg/ml; **e** treated at 1.56 µg/ml; **f** treated at 0.39 µg/ml)

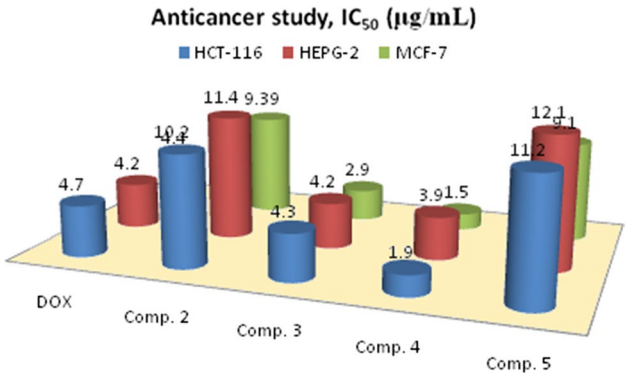

Fig. 9 Anticancer activity of the compounds (IC_{50} values)

In vitro antioxidant activity

The scavenging ability determines the antiradical power of an antioxidant. Here, the free radical scavenging activity evaluation is carried out to determine the antioxidant activity of all the tested ternary Ni(II) complexes at 5, 10, 20, 40, 80, 160, 320 and 640 µg concentrations by measuring the decrease in the absorbance of DPPH at 517 nm (Bou et al. 2013). Ascorbic acid is used as a standard drug. The absorbance has decreased when DPPH radical with purple color is scavenged by an antioxidant, through the donation of hydrogen to form a stable yellow color DPPH molecule (Mohapatra et al. 2019b; Arulpriya et al. 2012). The results of DPPH radical scavenging analysis can be seen in Figs. 10 and 11 and it displayed the dose–response curve of DPPH radical scavenging activity of ternary Ni(II) complexes compared with ascorbic acid. It was observed that at the lowest concentration (5 µg), the antioxidant activity of ascorbic acid was found to be 12.98%, but this value is increased to 14.71% for comp. 3. Meanwhile, this percentage is decreased in the range of 9.58- 10.19% `in the other mixed ligand complexes.

Molecular docking studies

The choice of tyrosine kinase PDB ID: 1M17 (Epidermal Growth Factor Receptor tyrosine kinase domain with 4-anilinoquinazoline inhibitor erlotinib) as a biological target for the study of the possible antitumor activity is due to the existing crystallographic model co-crystallized with a derivative of 4-anilinoquinazoline (Fig. S1). Based on the results of molecular docking the following data were calculated:

- the scoring function indicating the enthalpy contribution to the value of the free energy of binding (Affinity DG) for the best conformational positions (Table 3).
- the values of the free energy of binding and binding constants (EDoc kcal/mol and Ki mM (millimolar)) for a specific conformational position of the ligand; they allow assessing the stability of complexes formed between ligands and the corresponding receptor (Table 4).

It may be assumed that the inhibitory activity of the tested compounds relative to the tyrosine kinase receptor (PDB ID: 1M17) is actualized by forming complexes

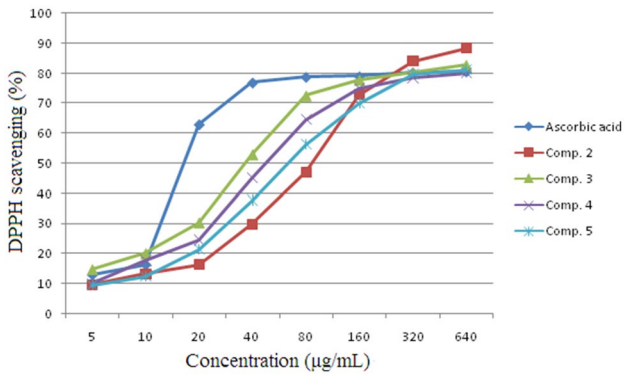

Fig. 10 Antioxidant activity of ascorbic acid and ternary Ni(II) complexes using DPPH scavenging

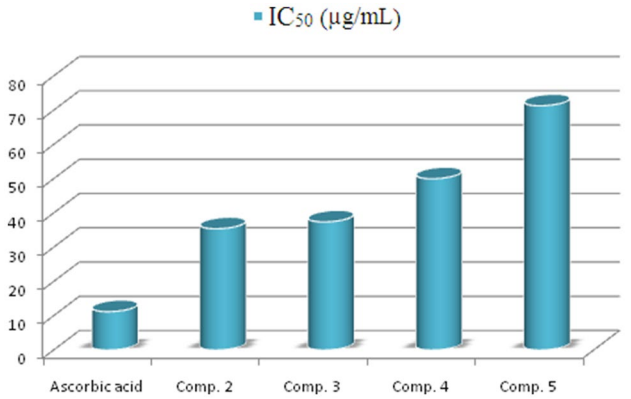

Fig. 11 Antioxidant activity of the compounds using DPPH scavenging

between them. Their stability is provided mainly due to the energy favorable geometric location of ligands in the active center of the acceptor, intermolecular electrostatic and donor–acceptor interactions and formation of hydrogen bonds. The thermodynamic probability is noticed by negative values of the scoring function (Affinity DG, kcal/mol), calculated values of the free energy of binding EDoc (kcal/mol), and binding constants Ki (mM/µM) (Table 5). To understand how the affinity of the drugs studied to the target, a detailed analysis of the geometric location of these molecules in the active site of the receptor was conducted.

Figure 12 displayed the ligand (Comp-1) superposition and the diagram of intermolecular interactions in the complex with the tyrosine kinase receptor (PDB ID: 1M17). The complex with the receptor is formed due to the hydrogen bonds between the hydroxyl group and the LEU764 residue with an interatomic distance of 2.76 Å, as well as with ALA719 with a distance of 2.50 Å, respectively. The π-cationic interaction occurs between the phenolic fragment of the molecule and LYS721 (interatomic distance –4.85 Å). The carbon-hydrogen interaction occurs between MET 769 and methyl with an interatomic distance of 3.24 Å. The additional stabilization of the complex is facilitated by π-Alk interactions occurring between the phenyl fragment and the LEU694, LEU820, LEU764, and VAL702 residues.

In the formation of the Comp-2 complex with tyrosine kinase (Fig. 13) hydrogen bonds are involved; they are formed between the crystal-bound water (oxygen atom of carboxyl group) and the ARG817 (2.35; 2.68 Å) and ASP831 (interatomic distance –2.84 Å) residues. The carbon-hydrogen bond occurs between MET769 and the methyl fragment (3.50 Å). There is the π–π interaction between PHE699 and the phenyl residue (4.13 Å). The π-anionic interaction occurs between the ASP831 residue and the phenyl fragment (interatomic distance is 3.20 and 3.55 Å, respectively). The complex of π-Alk interactions occurring between the phenyl ring and LEU694, VAL702 is stabilized. In the formation of the Comp-3 complex with tyrosine kinase the π-cation bond between ASP83, PHE699 and the phenyl fragment (3.90 Å and 4.59Å) is involved. The carbon-hydrogen bond occurs between THR766and the alkyl inclusion (3.72 Å) and this bond is fixed between LEU764 and the alkyl inclusion of the molecule (3.58Å). The complex of π–π, π-Alk and Alk interactions occurring between the phenyl ring and LYS721, LEU894, PHE 699 is stabilized (Fig. 13).

When a complex is formed between Comp-4 and the tyrosine kinase receptor, there is a hydrogen bond due to the oxygen atom of the carbonyl group and the CYS751 residue (interatomic distance—2.87 Å). Electrostatic interactions occur between the Nitrogen atom of the amino group and GLU738 (4.94 Å) and ASP831 (5.24 Å). There is the π-σ bond between the phenyl fragment and VAL702 (interatomic distance—3.94 Å). The carbon-hydrogen bonds are formed between the methyl fragment and PRO770 (3.80 Å) MET769 (3.78 Å). The additional stabilization of the complex is facilitated by π-Alk interactions between the phenyl fragment and the LEU820, VAL702, and LEU694 residues, respectively (Fig. 13).

When a complex is formed between Comp-5 and the tyrosine kinase receptor, there is a hydrogen bond due to the oxygen atom of the crystal-bound water and this connection occurs between the histidine fragment (nitrogen atom of the amino group) and the ARG817 residue (interatomic distance—2.12 Å and 2.16Å). Carbon hydrogen bonds arise between the alkyl moieties of the molecule and LEU761 (3.54Å), THR761 (3.15 Å) and ALA719 (3.75 Å). The appearance of the complex is facilitated by the π-anion and π-cation interactions with phenyl fragments and ASP831 residues with interatomic distances of 3.92 Å and 3.30 Å. The pi-sulfur bond is formed between the imidazole histidine cycle and the residue CYS773 (5.46 Å). Additionally stabilize the complex π–π, π-Alk interactions

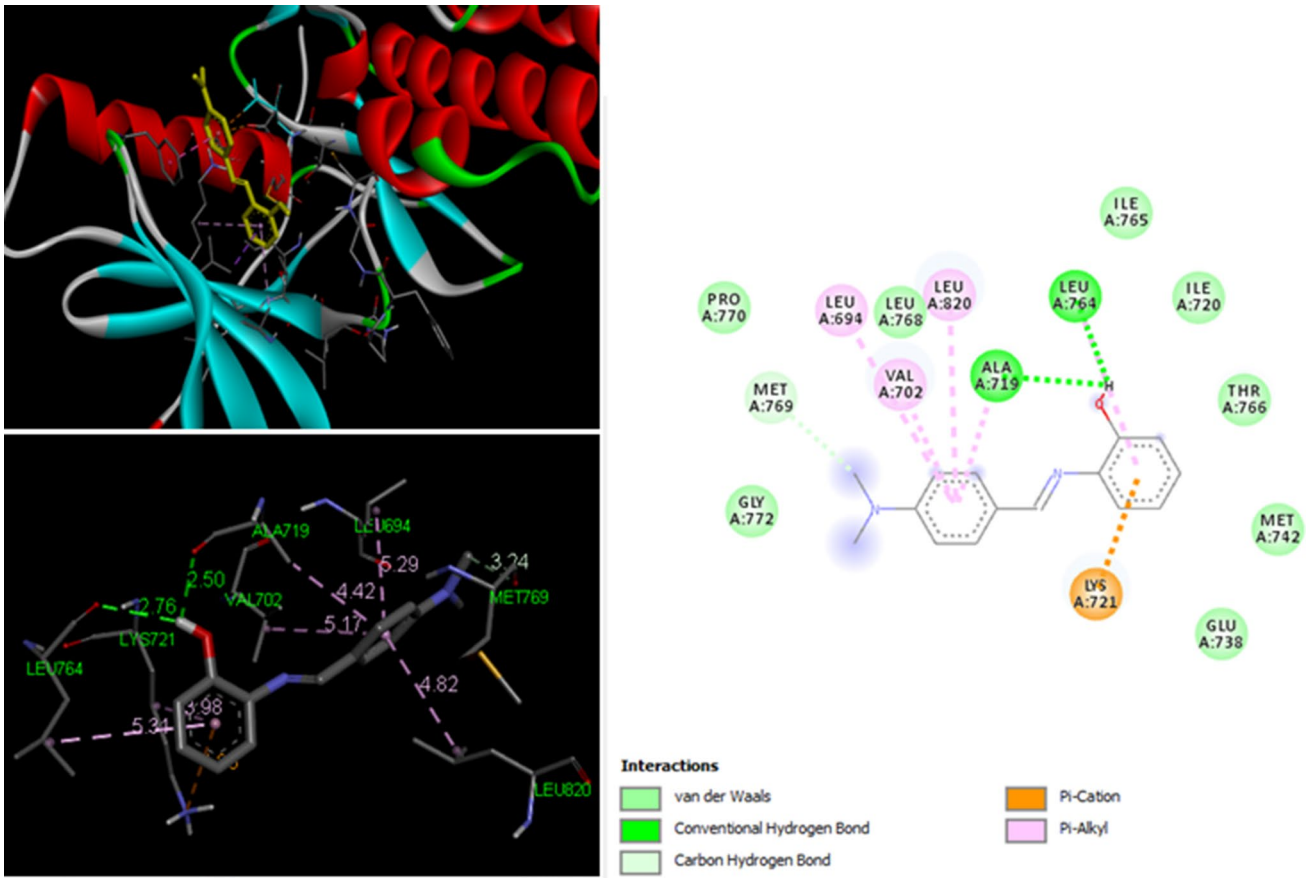

Fig. 12 The Ligand superposition and the diagram of intermolecular interactions in the complex with tyrosine kinase receptor (PDB ID: 1M17)

arising between aromatic fragments of the chelate complex and amino acid residues of PHE 699, VAL702 and LYS721 (Fig. 13). Taking into account the detailed analysis of the location of the molecules tested in the active site of the tyrosine kinase receptor, the formation of a number of intermolecular interactions between them, negative values of scoring functions and calculated values of binding constants, it can be concluded that the presence of nickel in the molecule contributed to an increase in the affinity for the specified biological target.

Table 3 Affinity DG values for 9 conformational positions of the test compounds in combination with the enzyme tyrosine kinase (PDB ID: 1M17)

No.	Afinity DG, kcal/mol				
	Comp. 1	Comp. 2	Comp. 3	Comp. 4	Comp. 5
1	−7.7	−9.4	−10.5	−9.2	−9.1
2	−7.7	−8.7	−8.4	−9.0	−8.1
3	−7.6	−8.5	−8.3	−8.4	−8.1
4	−7.1	−8.2	−8.0	−8.4	−8.0
5	−6.9	−8.1	−8.0	−8.4	−7.9
6	−6.6	−7.8	−7.5	−8.2	−7.9
7	−6.5	−7.8	–	−8.2	−7.8
8	−6.4	−7.7	–	−8.2	−7.5
9	−6.4	−7.7	–	−8.1	−7.5

Electrostatic potential analysis

The electrostatic potential surfaces of the Schiff base ligand and $[NiL1L5(H_2O)_2]2H_2O$ complex were executed by applying GAUSSIAN 09 platform. This framework is useful to understand the receptive behavior of a compound. From the molecular surface plot, the negative part of the electron cloud shows as nucleophilic centers, but the positive part of the electron cloud shows the potential electrophile sites. For clear understanding the different visible mode of ESP plots (Figs. S2 and S3) showed the molecular size, molecular shape and electrostatic potential activity. In the ligand, the amino nitrogen and hydroxy oxygen centers showed high negative electron potential locality. The electrostatic potential plot of $[NiL1L5(H_2O)_2]2H_2O$ was a predominance of the green region which clearly explained the complex is halfway potential electron

Table 4 Values of the free energy of binding and binding coefficients of the test antitumor agents in combination with the enzyme tyrosine kinase (PDB ID: 1M17)

No.	Comp. 1		Comp. 2		Comp. 3		Comp. 4		Comp. 5	
	EDockcal/mol	Ki mM/ μMmillimolar/ micromolar	EDockcal/mol	Ki mM/μMmillimolar/ micromolar	EDockcal/mol	Ki mM/ μMmillimolar/ micromolar	EDockcal/mol	Ki mM/ μMmillimolar/ micromolar	EDockcal/mol	Ki mM/ μMmillimolar/ micromolar
1	− 4.20	841.13 μM	− 3.99	1.19 mM	− 5.33	124.12 μM	− 4.53	477.58 μM	− 4.30	704.37 μM
2	− 3.42	3.11 mM	− 6.13	32.04 μM	− 4.64	394.51 μM	− 3.79	1.65 mM	− 4.69	366.56 μM
3	− 5.18	158.29 μM	− 4.08	1.02 mM	− 5.24	145.02 μM	− 4.60	426.31 μM	− 4.00	1.16 mM
4	− 3.69	1.97 mM	− 4.00	1.17 mM	− 5.50	93.51 μM	− 4.85	278.16 μM	− 4.55	463.30 μM
5	− 5.07	192.65 μM	− 4.73	340.10 μM	− 6.68	12.66 μM	− 3.68	2.01 mM	− 4.37	626.94 μM
6	− 5.27	137.59 μM	− 4.80	301.65 μM	− 5.27	136.88 μM	− 4.04	1.09 mM	− 4.12	960.79 μM
7	− 3.93	1.31 mM	− 5.21	151.93 μM	− 4.84	282.59 μM	− 3.86	1.48 mM	− 4.08	1.02 mM
8	− 3.23	4.30 mM	–	–	− 5.00	215.51 μM	− 4.44	559.20 μM	− 4.22	803.19 μM
9	− 4.05	1.08 mM	–	–	− 6.01	39.28 μM	− 4.93	243.03 μM	− 4.96	233.10 μM
10	− 4.60	424.46 μM	–	–	− 5.27	137.41 μM	− 4.71	354.05 μM	− 4.00	1.17 mM

Table 5 Quantitative structure–activity relationship calculation for optimized ligand (HL_1)

Function	(Comp. 1) (2-(2-(2,4-dinitrophenyl)hydrazone methyl phenol
Surface area (Approx) ($Å^2$)	400.29
Surface area (Grid) ($Å^2$)	483.20
Volume ($Å^3$)	782.35
Hydration energy (Kcal/mole)	− 19.26
Log P	3.05
Refractivity ($Å^3$)	26.45
Polarizability ($Å^3$)	28.28
Mass (amu)	302.25
Total energy (kcal/mol)	− 87723.16
Dipole Moment (Debye)	0
Free energy (kcal/mol)	− 87723.16
RMS Gradient (kcal/Å mol)	0.49

distribution among two extreme color red and blue (Maurya et al. 2014, Khanna et al. 2020).

Mulliken charge population analysis

The entire atomic charges of the ligand and $[NiL1L5(H_2O)_2]2H_2O$ were obtained by Mulliken charge population analysis studies (Mulliken 1995). This analysis was performed by GAUSSIAN 09 platform with B3LYP/LANL2DZ basic set. Ultimately Mulliken graphical plots were obtained for both ligand and complex (Figs. 14, 15). If we analyze the plots, atoms color are clearly showed Mulliken values in the positive and negative form of charge. The Mulliken charge population analysis is providing absolute details about total charge density or an orbital density of ligand and complex.

QSAR analysis

The *Quantitative Structure–Activity Relationship* technique is a useful tool to predict the activity, reactivity and properties of the prepared molecules. The computation work was carried out with the help of HyperChem Professional 8.0.3 platform. At first, the ligand structure is optimized by (MM^+) force field, with semi-empirical PM3 methods. Further, the energy minimization method was fulfilling with Fletcher-Reeves conjugate gradient algorithm. The calculated log P value for the ligand (HL_1) is 3.05. The crucial role of the partition coefficient (log P) value is to describe the biological activity of the ligand, which may evaluate the permeability of the applied compound into the cell membrane (Padmanabhan et al. 2007). Few other necessary physical parameters such as surface

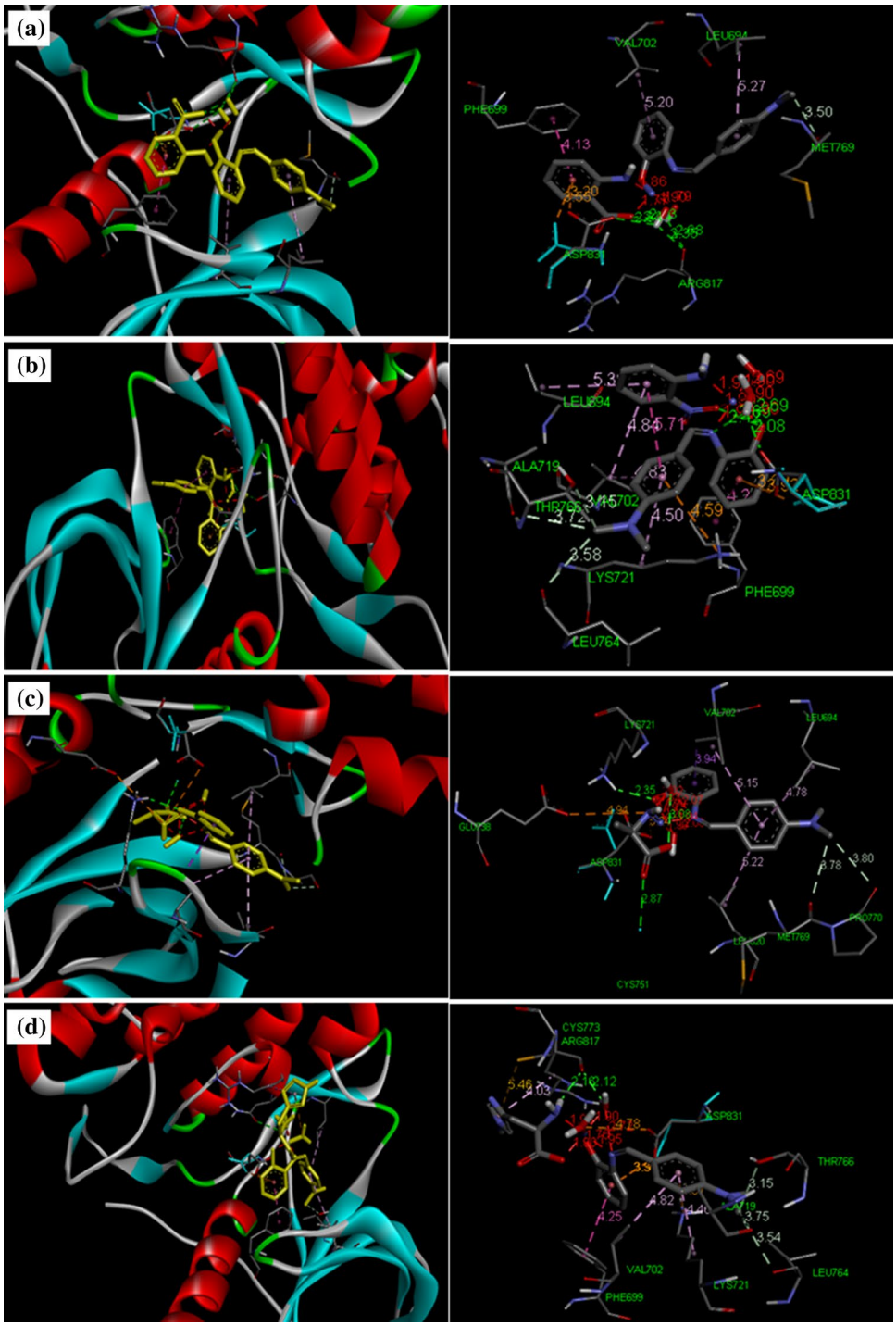

Fig. 13 The superposition in the complex with tyrosine kinase receptor (PDB ID: 1M17); **a** Comp-2, **b** Comp-3, **c** Comp-4, **d** Comp-5

area, volume, hydration energy, refractivity, polarizability, mass, total energy, free energy and RMS gradient were also evaluated to propose the reactivity of the ligand and represented in Table 5.

Conclusion

The anticancer and antioxidant properties of some ternary nickel complexes have been reported. The Schiff base acts as a primary ligand (HL_1) whereas; anthranilic acid (HL_2), 2-nitroaniline (HL_3), alanine (HL_4) and histidine (HL_5) act as secondary ligand or co-ligand. The anticancer activity of these compounds was studied against human colon

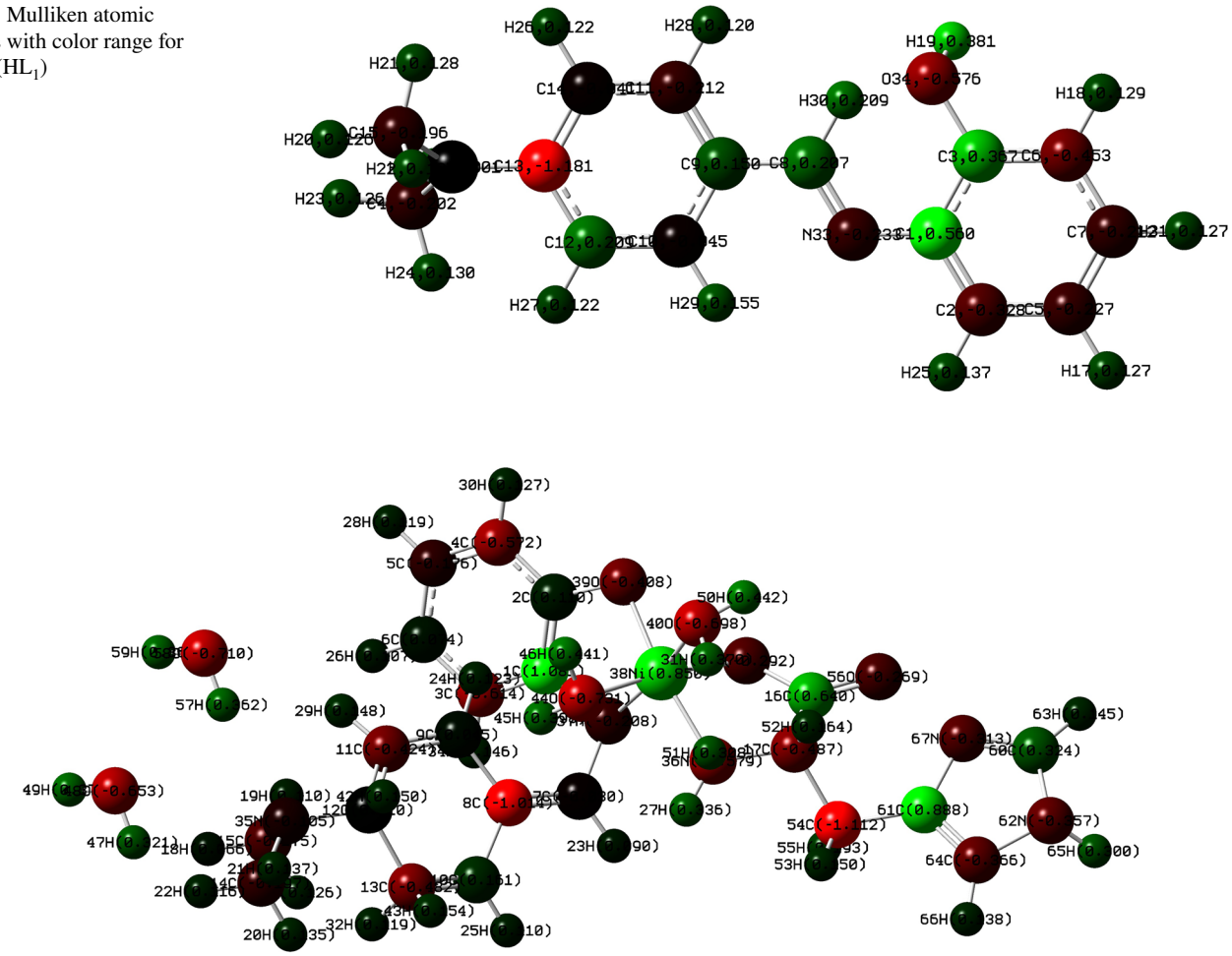

Fig. 14 Mulliken atomic charges with color range for ligand (HL_1)

Fig. 15 Mulliken atomic charges with color range for $[NiL1L5(H_2O)_2]2H_2O$

carcinoma (HCT-116), human hepatocellular liver carcinoma (HEPG-2) and human breast carcinoma (MCF-7) cell lines. The obtained data showed that compound 3 and 4 were found to be more potent against all cancer cell lines, whereas, compound 2 and 5 were found to be moderately active. The antioxidant activity of these compounds was evaluated using DPPH radical scavenging and compared with ascorbic acid. The DFT computations for these compounds were made to understand the mode of bonding. The molecular orbital energy gap between HOMO and LUMO for comp. 5 is established to be less than all the other compounds. From the energy comparison values it is prominently explained that the reactivity of comp. 5 is greater than all other compounds also. Moreover, a docking analysis using Autodock 4.2 software package was carried out against the tyrosine kinase receptor (PDB ID: 1M17). In addition, ESP and Mulliken charge population analysis were carried out using GAUSSIAN 09 platform. Furthermore, QSAR Analysis is reported to predict the activity and reactivity of the Schiff base ligand.

Acknowledgements The authors acknowledge the financial support through Researchers Supporting Project number (RSP-2020/147), King Saud University, Riyadh, Saudi Arabia. Dr. R. K. Mohapatra is grateful to the Principal, Government College of Engineering, Keonjhar for providing necessary facilities and support.

Compliance with ethical standards

Conflict of interest There are no conflicts to declare.

References

Ahamad MN et al (2020) Anticancer properties, apoptosis and catecholase mimic activities of dinuclear cobalt(II) and copper(II) Schiff base complexes. Bioorg Chem 95:103561. https://doi.org/10.1016/j.bioorg.2019.103561

Alassbaly FS, El-Ajaily MM, Ben-Gweirif SF, Maihub AA (2014) Preparation, spectroscopic investigation and biological activity of new mixed ligand chelates. J Chem Soc Pak 36(6):1034–1042

Alassbaly FS et al (2016) Chelation trends and antibacterial activity of some mixed ligand chelates. Saudi J Pathol Microbiol 1(2):29–35. https://doi.org/10.21276/sjpm.2016.1.2.1

Aljahdali MS, Elmalik YH, El-Reash GMA (2014) Synthesis of some transition metal complexes of novel 1-methylpyrazole-3- aldehyde-4-(2-pyridyl) thiosemicarbazone: Spectroscopic and in vitro biological activity studies. Eur J Chem 5(2):201–208. https://doi.org/10.5155/eurjchem.5.2.201-208.952

Arulpriya P, Lalitha P, Hemalatha S (2010) In vitro antioxidant testing of the extracts of Samanea saman (Jacq). Merr Der Chem Sin 1(2):73–79

Becke AD (1988) Correlation energy of an inhomogeneous electron gas: a coordinate-space model. Phys Rev A 88:1053–1062. https://doi.org/10.1063/1.454274

Becke AD (1993) Density-functional thermochemistry. III. The role of exact exchange. J Chem Phys 98(7):5648–5652. https://doi.org/10.1063/1.464913

Bou DD et al (2013) Chemical composition and cytotoxicity evaluation of essential oil from leaves of *Casearia Sylvestris*, its main compound α-zingiberene and derivatives. Molecules 18(8):9477–9487. https://doi.org/10.3390/molecules18089477

Chudzik M, Szlacheta IK, Krol W (2015) Triterpenes as potentially cytotoxic compounds. Molecules 20(1):1610–1625. https://doi.org/10.3390/molecules20011610

Drapak I et al (2019) QSAR-analysis of 1-[2-(R-phenylimino)-4-methyl-3-(3-[morpholine-4-yl]propyl)- 2,3-dihydro-1,3-thiazol-5-yl]ethane-1-one's derivatives as potential antioxidants. Pharmacia 66(1):33–40. https://doi.org/10.3897/pharmacia.66.e35083

El-ajaily MM, Alassbaly FS, Etorki AM, Maihub AA (2015) Mixed-Ligand Chelate Formation of Co(II), Ni(II), Cu(II) and Zn(II) Ions with Schiff Base as Main Ligand and Amino Acid as Co-Ligand. Int Res J Pure & Applied Chem 5(3):229–237. https://doi.org/10.9734/IRJPAC/2015/11786

El-ajaily MM et al (2018) Mixed ligand complexes containing schiff bases and their biological activities: a short review. Rasayan J Chem 11(1):166–174. https://doi.org/10.7324/RJC.2018.1111988

El-ajaily MM et al (2019) Transition metal complexes of (E)-2((2-hydroxybenzylidene) amino-3-mercaptopropanoic acid: XRD, anticancer, molecular modeling and molecular docking studies 4:9999–10005. https://doi.org/10.1002/slct.201902306

El-Barasi NM et al (2020) Synthesis, structural investigations and antimicrobial studies of hydrazone based ternary complexes with Cr(III), Fe(III) and La(III) ions. J Saudi Chem Soc 24:492–503. https://doi.org/10.1016/j.jscs.2020.04.005

El-Saghier AM, Abd El-Halim HF, Abdel-Rahman LH, Kadry A (2019) Green synthesis of new trizole based heterocyclic amino acids ligands and their transition metal complexes. Characterization, kinetics, antimicrobial and docking studies. Appl Organomet Chem 33:e4641. https://doi.org/10.1002/aoc.4641

Fathima SSA, Meeran MMS, Nagarajan ER (2019) Synthesis of novel (E)-2-((anthracen-9-ylmethylene)amino) pyridin-3-ol and its transition metal complexes: Multispectral characterization, biological evaluation and computational studies. J Mol Liq 279:177–189. https://doi.org/10.1016/j.molliq.2019.01.101

Frisch MJ et al (2009) GAUSIAN 09. Gaussian Inc., Wallingford

Gaber M, Khedr AM, Elsharkawy M (2017) Characterization and thermal studies of nano-synthesized Mn(II), Co(II), Ni(II) and Cu(II) complexes with adipohydrazone ligand as new promising antimicrobial and antitumor agents. Appl Organomet Chem. https://doi.org/10.1002/aoc.3885

Gaber M, El-Baradie K, El-Wakiel N, Hafez S (2019) Synthesis and characterization studies of 3-formyl chromone Schiff base complexes and their application as antitumor, antioxidant and antimicrobial. Appl Organometal Chem. https://doi.org/10.1002/aoc.5348

GaussView 5.0, (2009) Gaussian Inc., Wallingford, CT, USA 2009.

Govindarajan M, Periandy S, Carthigayen K (2012) FT-IR and FT-Raman spectra, thermo dynamical behavior, HOMO and LUMO, UV, NLO properties, computed frequency estimation analysis and electronic structure calculations on a-bromotoluene. Spectrochim Acta A 97:411–422. https://doi.org/10.1016/j.saa.2012.06.028

Hay PJ, Wadt WR (1985a) Ab Initio effective core potentials for molecular calculations. Potentials for the transition metal atoms Sc to Hg. J Chem Phys 82(1):270–283. https://doi.org/10.1063/1.448799

Hay PJ, Wadt WR (1985b) Ab Initio effective core potentials for molecular calculations. Potentials for main group elements Na to Bi. J Chem Phys 82:284–298. https://doi.org/10.1063/1.448800

Hay PJ, Wadt WR (1985c) Ab initio effective core potentials for molecular calculations potentials for K to Au including the outermost core orbitals. J Chem Phys 82:299–310. https://doi.org/10.1063/1.448975

Kaim W, Schwederski B (1996) Bioinorganic chemistry: inorganic elements of life. Wiley, London, p 39

Kavitha P, Reddy KL (2016) Pd(II) complexes bearing chromone based Schiff bases: Synthesis, characterisation and biological activity studies. Arab J Chem. https://doi.org/10.1016/j.arabjc.2013.06.018

Khanna L, Singhal S, Jain SC, Khanna P (2020) Spiro-indole-coumarin hybrids: synthesis, ADME, DFT, NBO studies and in silico screening through molecular docking on DNA G-quadruplex. Chemistryselect 5:3420–3433. https://doi.org/10.1002/slct.201904783

Lee C, Yang W, Parr RG (1988) Development of the Colic-Salvetti correlation-energy formula into a functional of the electron density. Phys Rev B 37:785–789. https://doi.org/10.1103/PhysRevB.37.785

Maihub AA, Alassbaly FS, El-Ajaily MM, Etorki AM (2014) Modification on synthesis of mixed ligand chelates by using Di- and trivalent transition metal ions with schiff base as primary ligand. Green Sustain Chem 4:103–110. https://doi.org/10.4236/gsc.2014.43015

Mantasha I et al (2019) Synthesis, crystal structures, photoluminescence, magnetic and antioxidant properties, and theoretical analysis of Zn(II) and Cu(II) complexes of an aminoalcohol ligand supported by benzoate counter anions. New J Chem 43:622–633. https://doi.org/10.1039/C8NJ04122A

Maurya RC, Malik BA, Mir JM, Sharma AK (2014) Synthesis, characterization, thermal behavior, and DFT aspects of some oxovanadium(IV) complexes involving ONO-donor sugar Schiff bases. J Coordinat Chem 67(18):3084–3106. https://doi.org/10.1080/00958972.2014.959508

Mohapatra RK, Dash M, Mishra UK, Mahapatra A, Dash DC (2014) Synthesis, spectral characterization, and fungicidal activity of transition metal complexes with benzimidazolyl-2-hydrazones of glyoxal, diacetyl, and Benzil. Synth React Inorg Metal-Org Nano-Met Chem 44:642–648. https://doi.org/10.1080/15533174.2013.776592

Mohapatra RK, Das PK, El-ajaily MM, Mishra U, Dash DC (2018a) Synthesis, spectral, thermal, kinetic and antibacterial studies of transition metal complexes with benzimidazolyl-2-hydrazones of *o*-hydroxyacetophenone, *o*-hydroxybenzophenone and *o*-vanillin. Bull Chem Soc Ethiop 32(3):437–450. https://doi.org/10.4314/bcse.v32i3.3

Mohapatra RK, Das PK, Pradhan MK, Maihub AA, El-ajaily MM (2018b) Biological aspects of Schiff base–metal complexes derived from benzaldehydes: an overview. J Iran Chem Soc 15:2193–2227. https://doi.org/10.1007/s13738-018-1411-2

Mohapatra RK et al (2019a) Recent advances in urea- and thiourea-based metal complexes: biological, sensor, optical, and corrosion inhibition studies. Comment Inorg Chem 39(3):127–187. https://doi.org/10.1080/02603594.2019.1594204

Mohapatra RK, Sarangi AK, Azam M et al (2019b) Synthesis, structural investigations, DFT, molecular docking and antifungal studies of transition metal complexes with benzothiazole based Schiff base ligands. J Mol Struct 1179:65–75. https://doi.org/10.1016/j.molstruc.2018.10.070

Mulliken RS (1955) Electronic population analysis on LCAO-MO molecular wave functions. J Chem Phys 23:1833–1840. https://doi.org/10.1063/1.1740588

National Committee for Clinical Laboratory Standards (2000) NCCLS approval standard document M2-A7. Vilanova, PA

Padmanabhan J, Parthasarathi R, Subramanian V, Chattaraj P (2005) Molecular structure, reactivity, and toxicity of the complete series of chlorinated benzenes. J Phys Chem 109(48):11043–11049. https://doi.org/10.1021/jp0538621

Patal S (1970) The chemistry of carbon nitrogen double bond. Interscience Publishers Inc., New York, p 1970

Pearson RG (1989) Absolute electronegativity and hardness: applications to organic. J Org Chem 54(6):1423–1430. https://doi.org/10.1021/jo00267a034

Pearson RG (1993) The principle of maximum hardness. Acc Chem Res 26:250–255. https://doi.org/10.1021/ar00029a004

Rao TP, Reddy MLP, Pillai AR (1998) Application of ternary and multicomponent complexes to spectrophotometric and spectrofluorimetric analysis of inorganics. Talanta 46:765–813. https://doi.org/10.1016/S0039-9140(97)00262-2

Sama F et al (2017) Amino alcohols and benzoates-Friends or foes? Tuning nuclearity of Cu(II) complexes, structures, magnetism, DFT and TD-DFT studies, and catecholase like activities. Dalton Trans 46:9801–9823. https://doi.org/10.1039/C7DT01571B

Sarangi AK, Mahapatra BB, Sethy SK (2018) Synthesis and characterization of tetranuclear metal complexes with an octadentate azodye ligand. Chem Afr 1:17–28. https://doi.org/10.1007/s42250-018-0002-z

Sarangi AK, Mahapatra BB, Mohapatra RK et al (2020) Synthesis and characterization of some binuclear metal complexes with a pentadentate azodye ligand: an experimental and theoretical study. Appl Organometal Chem 34:e5693. https://doi.org/10.1002/aoc.5693

Shier WT (1991) Mammalian cell culture on $5 a day: a lab manual of low cost methods. University of the Philippines, Los Banos, p 1991

Sigel H (1975) Ternary Cu^{2+} complexes: stability, structure, and reactivity. Angew Chem Int Ed 14:394–402. https://doi.org/10.1002/anie.197503941

Skehan P et al (1990) New colorimetric cytotoxicity assay for anticancer-drug screening. J Natl Cancer Inst 82(13):1107–1112. https://doi.org/10.1093/jnci/82.13.1107

Yousef TA, El-Reash GMA, Rakha TH, El-Ayaan U (2011) First row transition metal complexes of (E)-2-(2-(2-hydroxybenzylidene) hydrazinyl)-2-oxo-N-phenylacetamide complexes. Spectrochim Acta A 83(1):271–278. https://doi.org/10.1016/j.saa.2011.08.030

Yousef TA, Rakha TH, El-Ayaan U, El-Reash GMA (2012a) Synthesis, spectroscopic characterization and thermal behavior of metal complexes formed with (Z)-2-oxo-2-(2-(2-oxoindolin-3-ylidene) hydrazinyl)- N-phenylacetamide (H_2OI). J Mol Struct 1007:146–157. https://doi.org/10.1016/j.molstruc.2011.10.036

Yousef TA, El-Reash GMA, El-Morshedy RM (2012b) Quantum chemical calculations, experimental investigations and DNA studies on (E)-2-((3-hydroxynaphthalen-2-yl)methylene)-N-(pyridin-2-yl) hydrazinecarbothioamide and its Mn(II), Ni(II), Cu(II), Zn(II) and Cd(II) complexes. Polyhedron 45:71–85. https://doi.org/10.1016/j.poly.2012.07.041

Yousef TA, El-Reash GMA, El-Morshedy RM (2013) Structural, spectral analysis and DNA studies of heterocyclic thiosemicarbazone ligand and its Cr(III), Fe(III), Co(II) Hg(II), and U(VI) complexes. J Mol Struct 1045:145–159. https://doi.org/10.1016/j.molstruc.2013.03.060